ISSN 1547-4771, Physics of Particles and Nuclei Letters, 2016, Vol. 13, No. 1, pp. 140–148. © Pleiades Publishing, Ltd., 2016.
Original Russian Text © E.K. Kozlova, V.A. Sergunova, E.A. Krasavin, A.V. Boreyko, A.V. Zavialova, A.P. Kozlov, A.M. Chernysh, 2016, published in Pis'ma v Zhurnal Fizika Elementarnykh Chastits i Atomnogo Yadra, 2016.

RADIOBIOLOGY, ECOLOGY AND NUCLEAR MEDICINE

Local Defects in the Nanostructure of the Membrane of Erythrocytes upon Ionizing Radiation of Blood

E. K. Kozlova[a, b], V. A. Sergunova[a], E. A. Krasavin[c], A. V. Boreyko[c], A. V. Zavialova[a], A. P. Kozlov[b], and A. M. Chernysh[a, b]

[a] *Negovsky Scientific Research Institute of General Reanimatology, Moscow, Russia*
[b] *Sechenov First Moscow State Medical University, Moscow, Russia*
[c] *Joint Institute for Nuclear Research, Dubna, Russia*
e-mail: waterlake@mail.ru
Received April 11, 2015

Abstract—The purpose of the study is to investigate local topological defects in the erythrocyte membranes resulting from the ultraviolet (UV) radiation of blood in vitro. Biological effects in the erythrocytes after exposure to UV radiation at a wavelength of 254 nm are equivalent to those after γ radiation. It has been shown that oxidative processes developing in a suspension upon UV radiation result in the disruption of the nanostructure of the membranes of erythrocytes. In the experiments, typical topological defects in the membrane nanostructure were observed. The parameters of the defects differed from the characteristics of the nanostructure of the control cell membrane without irradiation. The characteristic dimensions of the topological defects are commensurate with the size of the spectrin matrix. As a result of the exposure to the UV radiation, polymorphism of the erythrocytes was observed.

DOI: 10.1134/S1547477116010131

The effect of ionizing radiation on biological objects is an urgent problem of radiobiology and nuclear physics. Ionizing radiation induces damage to subcellular structures and cell membranes upon long space flights, radiation and radionuclide therapy, during the sterilization of donor blood, and during anthropogenic disasters [1–4]. The study of the effect of radiation on membranes of red blood cells (erythrocytes) is of peculiar interest.

It has been shown earlier using calibrated electroporation that in the erythrocyte membrane latent damages in the nanostructure take place within a wide range of doses. These processes were studied for γ radiation, heavy metals (boron ions), and beams of accelerated electrons [5–7]. The appearance of the defects in the membrane nanostructure was accompanied by impairments in the ion exchange and, as a result, by changes in the cell morphology. It was shown that, upon the sterilization of donor blood or erythrocyte suspension using ionizing radiation within doses reaching tens of kGy, the haematological parameters of the blood changed [8]. As a result, the gas exchange between the blood and tissues was impaired and pathophysiological processes developed in the organism as a whole [9, 10].

The detection and study of peculiarities of structural changes of biological membranes upon ionizing radiations is complicated due to the requirement for a large number of experiments either with radioactive sources or accelerators. At the same time, a number of regularities could be observed in in vitro experiments using ultraviolet (UV) radiation. The biophysical justification for this is that the effect of UV radiation on blood as well as that of ionizing radiation induces the formation of reactive oxygen species and the enhancement of oxidative processes both in hemoglobin molecules and in molecules of the membranes of the red blood cells [9]. Thus, UV radiation is an adequate alternative to γ radiation, both in clinical cases and in vitro studies [1, 11–13]. The biological consequences in erythrocytes subjected to UV radiation at a wavelength of $\lambda = 254$ nm are equivalent to the effects upon γ radiation [8, 11].

A promising method for studying membrane topology upon any kind of exposure is atomic force microscopy (AFM) [14–18]. AFM makes it possible to record the sizes of biological structures down to 0.1 nm. Using AFM, it was shown that it is local changes in the membrane nanostructure that trigger the mechanism of alterations in the shape of red blood cells during the long-term storage of donor blood, intoxication, and massive blood loss [16, 17, 19–21]. AFM could be used as an effective method for analyzing the nanostructure of membranes of red blood cells subjected to ionizing radiation in radiobiology and nuclear medicine. This work is aimed at studying local topological defects in erythrocyte membranes appearing due to the UV radiation of blood in vitro.

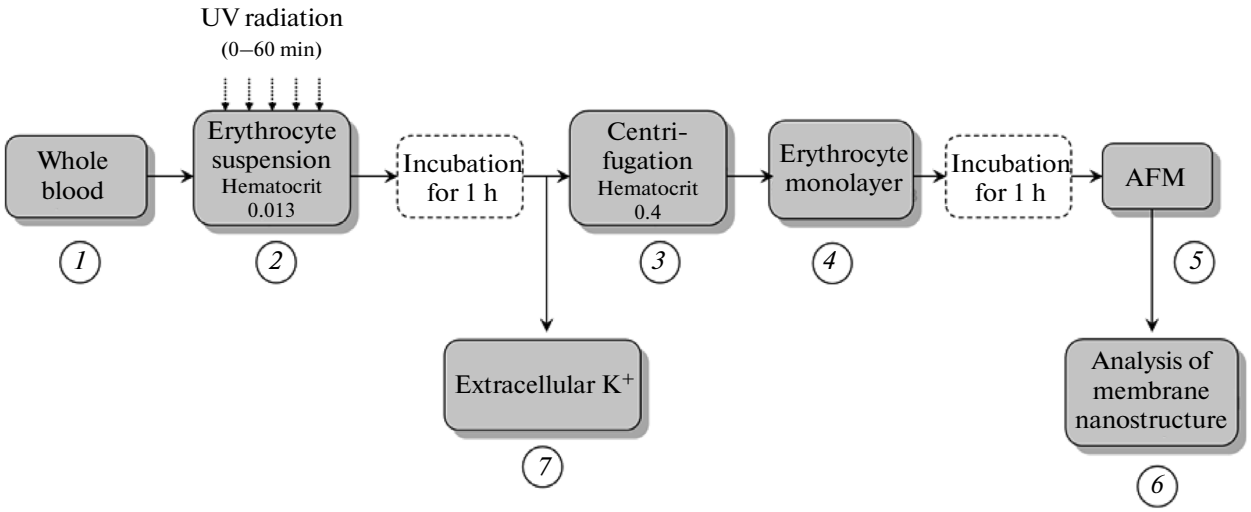

Fig. 1. Scheme of the experiment. (*1*) Preparation of a suspension, (*2*) exposure to UV radiation, (*3*) centrifugation, (*4*) preparation of erythrocyte smears, (*5*) atomic force microscopy, (*6*) analysis of membrane nanostructure, and (*7*) measurement of the concentration of ions of extracellular potassium.

MATERIALS AND METHODS

Experiments were performed according to a scheme given in Fig. 1.

1. Blood sampling was performed using Microvette tubes with EDTA (Sarstedt AG and Co., Germany) during the preventive examination of four male donors 27–34 years in age. In the study, the blood groups 0, A, B, and AB were used. According to the requirements of the Ethics Committee of the Negovsky Scientific Research Institute of General Reanimatology, all the donors gave their consent to participate in the study.

2. Whole blood significantly absorbs UV radiation at a wavelength of $\lambda = 254$ nm. To ensure the homogeneity of irradiation of erythrocytes along the entire volume (10 mL), the whole blood was diluted in a phosphate buffer (PBS pH 7.4) up to a hematocrit of 0.013. For this, medical plastic cuvettes were filled with 24 mL of the buffer solution and supplemented with 800 μL of the whole blood (hematocrit of 0.4). As a result, the suspension hematocrit was 0.013. Out of the suspension obtained, 12 mL was not subjected to radiation (control). The other 12 mL of the erythrocyte suspension was subjected to UV radiation in vitro. The storage time of the suspension was 1 h.

As a source of the ultraviolet radiation, an ultraviolet radiation source (ORUBp-3-3, KRONT, Russia) was used. The irradiation wavelength was $\lambda = 254$ nm, the photon energy was $E = 4.8$ eV, and the bactericidal flux of the lamp was $\Phi = 4.8$ W. The area of the suspension surface irradiated in a cuvette was $S = 12$ cm^2.

The dose absorbed upon the UV radiation of the erythrocyte suspension was assessed by a Fricke dosimeter [22]. The measure of the dose absorbed was the concentration of the salt of ferric iron Fe^{3+} that was formed upon the irradiation of an aqueous solution by the salt of ferrous iron Fe^{2+} under the effect of the radiolysis products. The concentration of the salt of ferric iron was measured using a spectrophotometric method at a wavelength of $\lambda = 304$ nm (a Unico 2800 spectrophotometer, United States). Upon an increase in the dose of UV radiation, the concentration of Fe^{3+} increased and, correspondingly, the optical density of the solution increased.

The radiation dose was varied by changing the duration of the irradiation. The blood samples were irradiated for 0 (control), 5, 10, 20, 30, 40, and 60 min. For each dose of irradiation, an erythrocyte suspension was prepared individually. Each experiment was repeated thrice. The doses for the different durations of the UV exposure were assessed according to the optical density (in relative units). The correspondence of the duration of the irradiation and doses is given in Table 1.

3. For preparation of erythrocyte monolayers, the suspension hematocrit was reduced down to the initial one, 0.4. For this, the suspension irradiated was cen-

Table 1. Doses for different durations of irradiation

Duration of irradiation	Dose, rel. un
0	0
5	0.1
10	0.2
20	0.4
30	0.5
40	0.6
60	0.8

trifuged (a Hettich Mikro 220R centrifuge, Germany, 1000 rps, 5 min) and the supernatant liquid was removed.

4. Preparation of monolayers is an important stage for obtaining high-quality images of cells and nanostructures of their membranes using an atomic force microscope (AFM).

A cell monolayer on a glass slide was obtained by a V-Sampler device (Austria), for which 10 μL of this suspension were used.

For each radiation dose, three cell monolayers were prepared (1.5 × 1.5 cm). The monolayers were dried in air for 1 h at room temperature. With the purpose of excluding artifacts upon analyzing the membrane nanostructure, chemical fixing fluids were not used. The monolayers were prepared 1 h after the exposure of the suspension to UV radiation.

5. Images of the cells and their membranes were obtained using an atomic force microscope (AFM) (NTEGRA Prima, (NT–MDT, Russia) in semicontact mode with the number of points in each line of the image being 512 or 1024. NSG01 cantilevers were used (R = 10 nm, the elastic coefficient of the cantilever K = 5 N/m, the resonance frequency = 130 kHz).

6. Analysis of the cell morphology was performed according to three fragments of 100 × 100 μm in each monolayer. For each irradiation dose, 27 images were obtained, each having 60–100 cells. Each image had a number of different shapes of erythrocytes resulting from poikilocytosis. The total sample size was 11340 cells.

The study of the membrane nanostructure was carried out on typical cells present in a great number. For each dose, from 3 to 10 typical cells were chosen. On the surface of the membrane of each cell, 3–4 regions with a size from 1000 × 1000 nm to 2000 × 2000 nm were chosen and scanned. In total, 680 fragments of the cell membranes were analyzed in the study.

For processing the AFM images obtained, FemtoScan Online program software (Advanced Technologies Center, Moscow) was used. To obtain a detailed image of the membrane surface, the initial surface of the membrane was broken down into three components using a spatial Fourier transform. This approach was suggested and described in detail in our previous studies [15, 18].

7. The concentration of K^+ ions was measured using an I-510 ionometric converter (Akvilon, Russia). A KhS-K-001 potassium selective electrode (Sensornye sistemy, Russia) was used. Calibration curves of the dependence of the electrode potential on the concentration of potassium ions were obtained. As a result, the concentration of extracellular potassium was measured before and after exposure to UV radiation.

RESULTS AND DISCUSSION

Changes in the Morphology

The monolayer of the blood subjected to UV radiation had discocytes, stomatocytes, planocytes, echinocytes, spheroechinocytes, spherocytes, and membrane ghosts observed. Their percentage ratio depended on the dose of the UV radiation of the blood (Fig. 2).

Figure 2a gives AFM 2D images of cell monolayers with different durations of the irradiation of 0, 10, and 40 min. Figure 2d gives percentage ratios of cells of different shapes found in the suspension after UV exposure. The cells in the control (without radiation) are mainly planocytes and echinocytes-1 (Fig. 2a). This smear differs from the whole blood smear, which usually contains discocytes. The appearance in the control smear of planocytes and echinocytes-1 was due to the significant dilution of the whole blood by the buffer (almost by a factor of 30) and further centrifugation of the suspension up to the restoration of the initial hematocrit. After the irradiation in the monolayer (b), 65% of the cells were represented by echinocytes, 15% by planocytes, 9% by discocytes, 6% by spheroechinocytes, 3% by spherocytes, 2% by stomatocytes, and ghosts were almost absent. In the monolayer (c), 29% of the cells were represented by spherocytes, 28% by spheroechinocytes, 22% by ghosts, 18% by echinocytes, 2% by stomatocytes, 1% by planocytes, and discocytes were almost absent.

A change in the percentage ratio of different cell shapes illustrates the dynamic of their sequential transformation. For example, formation of echinocytes-2 is the next stage of cell transformation after the formation of echinocytes-1 and planocytes. Thus, at D = 0.2, the number of echinocytes-2 increases to 51% and the number of echinocytes-1 and planocytes decreases. However, upon a further increase in the dose up to D = 0.6, part of echinocytes-2 transforms into spheroechinocytes. Therefore, the number of echinocytes-2 decreases to 15% and the number of spheroechinocytes increases. Such a nonlinear change in the number of cell shapes indicates that the cell shape echinocyte-2 is intermediate between discocytes and spheroechinocytes.

Upon an increase in the duration of irradiation, the dynamics of transformation of cells into echinocytes and spherocytes was observed. Such a change in the morphology of blood cells could lead to a change in their functional state and deterioration of the gas-transport function.

A change in the Nanostructure of the Membrane Surface of Erythrocytes

To assess quantitative parameters of the topological defects, an AFM image of the membrane fragment was broken into first- and second-order surfaces using a spatial Fourier transform [18].

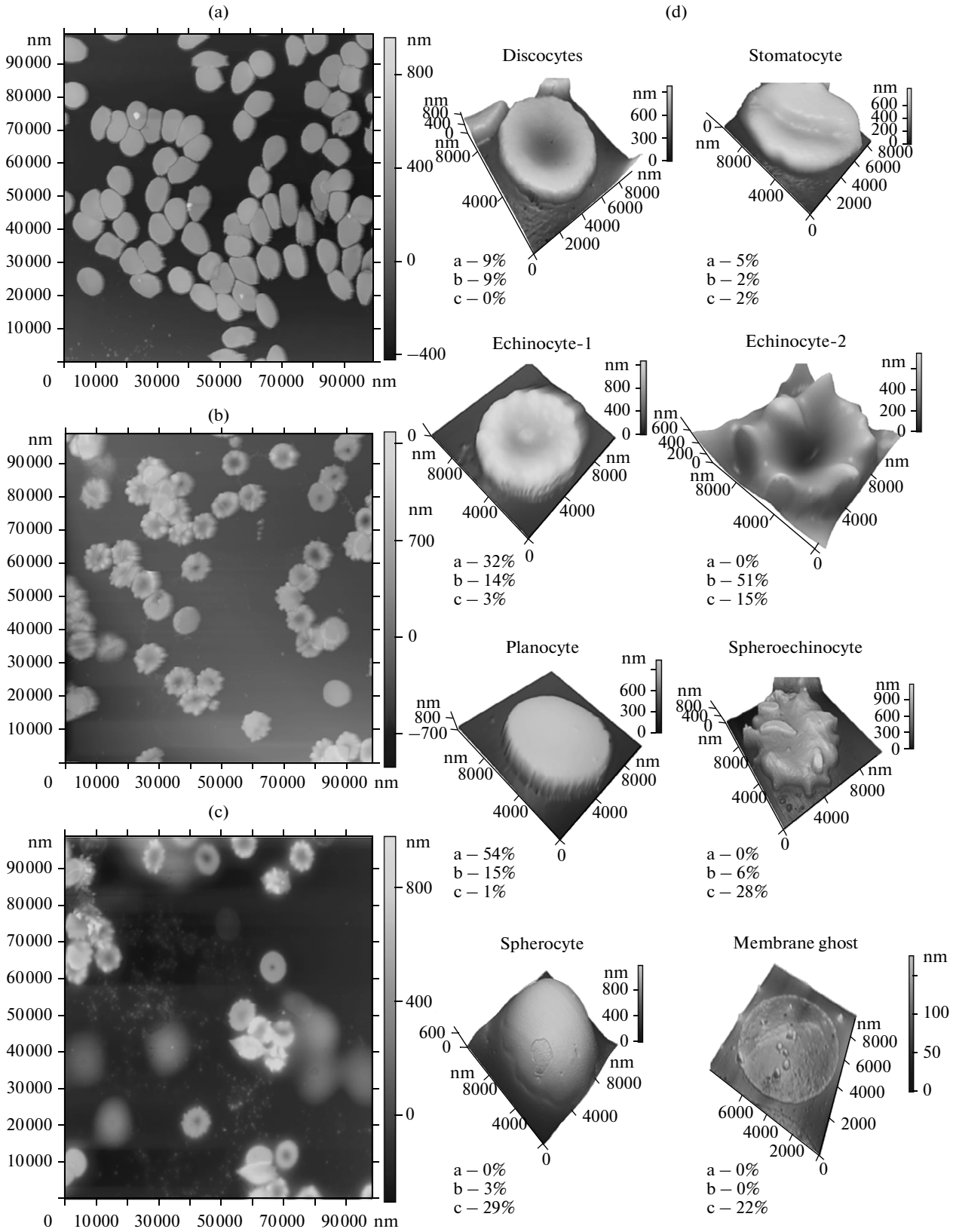

Fig. 2. Change in the percentage ratio of different shapes of the cells for different doses of UV radiation of an erythrocyte suspension. AFM 2D images of cell monolayers of 100 × 100 μm: (a) $D = 0$, control; (b) $D = 0.2$; and (c) $D = 0.6$ (d). Spatial distribution of the cells of different shapes in the smears (a–c). Duration of storage of the erythrocytes suspension after irradiation, $t_{storage} = 1$ h.

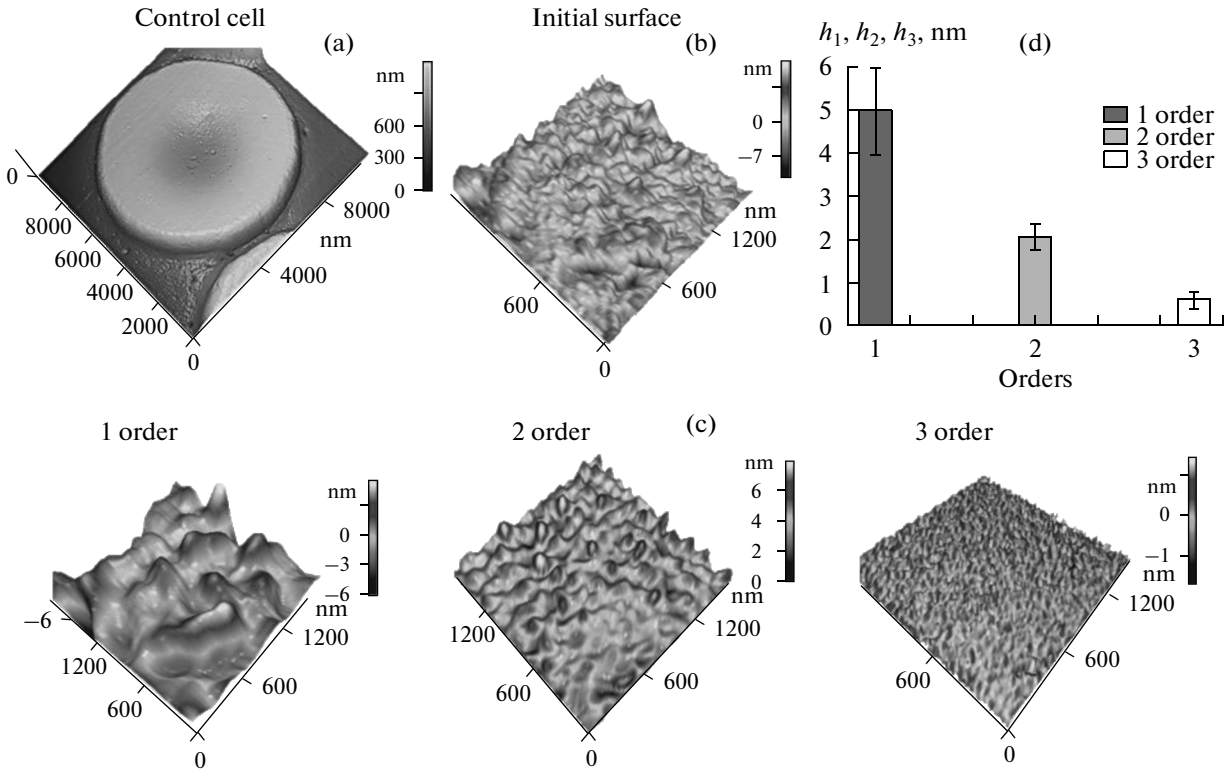

Fig. 3. AFM image of a control cell (a); nanosurface of a membrane fragment (b); first-, second-, and third-order surfaces (c); and histogram of the heights of these surfaces (d).

Figure 3 gives AFM images of a control cell (a), an initial region of the membrane (b), images of three components of the surface (first-, second-, and third-order surfaces) (c), and a histogram of heights of these surfaces (d). Summing up the surfaces given in Fig. 3c, the image of the initial surface is obtained (Fig. 3b).

Earlier it was shown that a change in the cell morphology begins with a change in the nanostructure of erythrocyte membranes. This takes place under the effect of chemical pharmaceutical drugs on blood [18, 19, 20] and during the long-term storage of donor blood [23, 24]. Different kinds of exposure induce specific topological defects in the membrane with pronounced characteristic spatial shapes and sizes [15, 18–20].

After the UV irradiation of the cell suspension, specific topological nanodefects in the structure of the membranes of the red blood cells were recorded. Herewith, two types A and B defects (Figs. 4, 5) were observed. The type A defects have ring-shaped nanocavities (Fig. 4). The type B defects represent a nanostructure in the form of a projecting ring (Fig. 5).

Figure 4a gives an AFM image of a cell with type A defects being observed on the membrane. The initial nanosurface of the membrane (Fig. 4b) was broken down into first-order (Fig. 4c) and second-order (Fig. 4e) surfaces. The corresponding profiles of these surfaces are given in Figs. 4d and 4f. The diameter of the type A topological defect is 600 ± 80 nm. The width of the type A topological defect is $L_2 = 170 \pm 40$ nm, which is comparable with the size of the spectrin tetramer.

The characteristic parameters of the surface of the ith order is the height h_i and spatial period L_i [18]. For comparison, the parameters of the nanostructure are given in Table 2.

At a dose from 0.2 to 0.8 (rel. un.), type A topological defects were observed in 25% of the cells (sample size is 500 cells). The number of these defects in a cell is 7 ± 5.

Type B topological defects represent a ring-shaped nanostructure projecting over the membrane surface. Figure 5a gives an AFM image of a cell with type B defects being observed on its membrane. The initial nanosurface of the membrane (Fig. 5b) was broken down into first-order (Fig. 5c) and second-order (Fig. 5e) surfaces. The corresponding profiles of these surfaces are given in Figs. 5d and 5f. The diameter of the type B topological defect is 1400 ± 600 nm.

The width of the type B topological defect was $L_2 = 90 \pm 20$ nm, which is comparable with the size of the spectrin dimer.

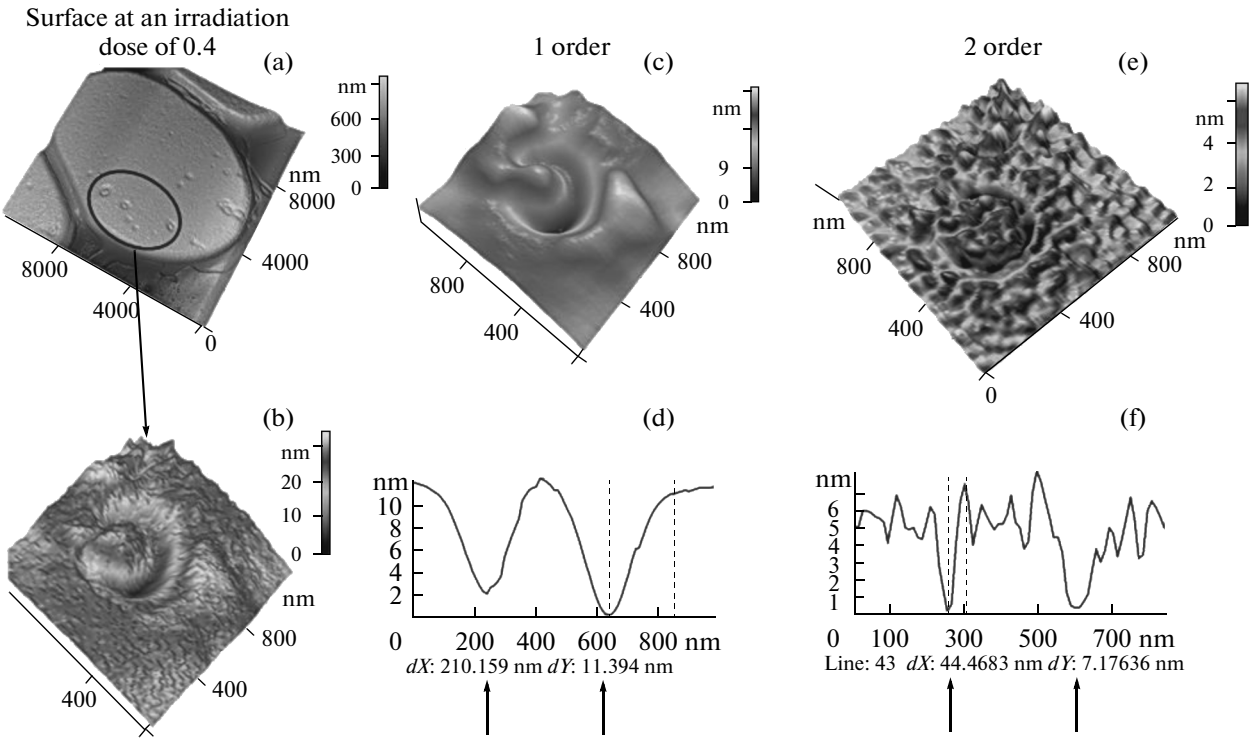

Fig. 4. Change in the nanostructure of an erythrocyte membrane after UV radiation, a topological defect in the nanostructure in the form of a circular nanocavity (type A), "vesiculation inside." An AFM 3D image of the cell with defects on the membrane surface of 10 × 10 μm at a dose of 0.4 (a), an AFM 3D image of 1 × 1 μm of the topological defect on the membrane surface (b), an AFM 3D image of the first-order surface (c) and the profile (d), and an AFM 3D image of the second-order surface (e) and the profile (f). Arrows indicate regions of the topological nanodefects.

The characteristic parameters of the nanostructure are given in Table 2.

Type B topological defects were observed in 8% of the cells at a dose from 0.2 to 0.8 rel. un. (the sample is 500 cells). The number of the defects per cell was 2 ± 1.

It follows from Table 2 that the heights of the first- and second-order surfaces differ approximately by a factor of 2 from the region of the defect when compared to the control surface.

Development of Oxidative Processes in the Membranes

To assess the intensity of the development of oxidative processes in the erythrocyte membranes after exposure to UV radiation, the concentration of extracellular potassium in the suspension was measured. With an increase in the radiation dose, the concentration of the extracellular potassium increased (Fig. 6) from 0.44 mM (in the control suspension, $D = 0$) to 1.32 mM (dose of 0.8). Figure 6 demonstrates typical cells and nanostructures of the surface for the corre-

Table 2. Parameters of first- and second-order nanosurfaces

	First order		Second order	
	h_1, nm	L_1, nm	h_2, nm	L_2,nm
Control	5 ± 1	800 ± 300	2.1 ± 0.3	100 ± 30
Type A defect	9 ± 3	600 ± 80	5.3 ± 1.2	170 ± 40
Type B defect	8.5 ± 1.5	1400 ± 600	5 ± 1	90 ± 20

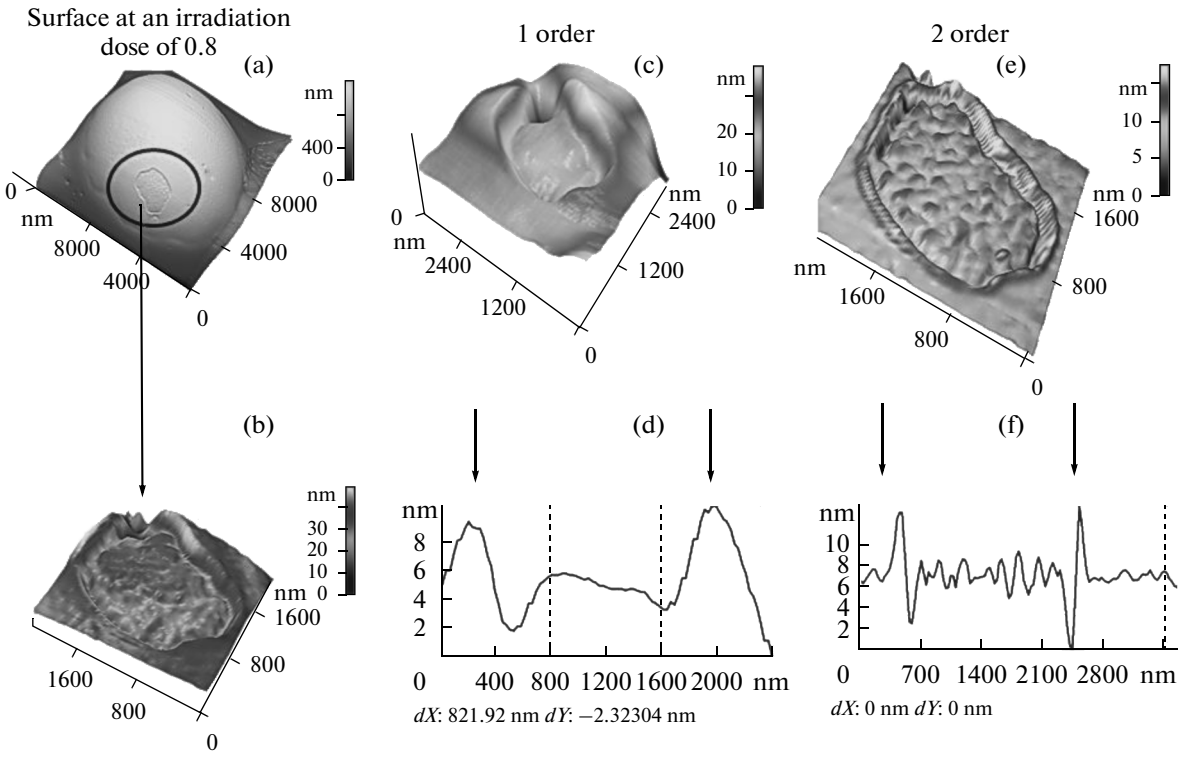

Fig. 5. Change in the nanostructure of an erythrocyte membrane after UV radiation, a topological defect in the nanostructure in the form of a ring projecting over the membrane surface (type B), "vesiculation outside." AFM 3D image of a cell with the defect on the membrane surface of 10 × 10 μm at a dose of 0.8 (a), AFM 3D image of 2000 × 2000 nm of the topological defect on the membrane surface (b), AFM 3D image of the first-order surface (c) and the profile (d), and AFM 3D image of the second-order surface (e) and the profile (f). Arrows indicate regions of the topological nanodefects.

sponding doses. It follows from Fig. 6 that, at doses of 0.6–0.8, intense potassium outflow into the suspension is observed, which correlates with a change in the membrane nanostructure and irreversible change in the cell morphology.

In the study presented, a model source of the exposure was represented by the UV radiation. Earlier [11] it was shown that such a model is adequate and comparable with the effect of γradiation up to high doses of 5–30 kGy [8]. Under the effect of UV radiation on blood, oxidative processes are activated and different ROSs are formed. At a wavelength of UV radiation less than 280 nm, the reaction of formation of radicals $H_2O \rightarrow H^{\cdot} + OH^{\cdot}$ takes place. Further different reactions are possible, e.g., $OH^{\cdot} + OH^{\cdot} \rightarrow H_2O_2$ [10, 25].

The final products of radiolysis of water under the effect of ionizing and UV radiation are the same. ROSs lead to the development of the chain reaction of lipid peroxidation [10]. As a result, in membrane lipids, a hydrophobic nonpolar bond L–H turns into a polar hydrophilic bond L–O–O–H. This results in the formation of local pores in the membrane and a change in the conditions of diffusion for molecules of water and ions and, on the whole, in the impairment of the ionic balance and cell morphology. ROSs also induce oxidation of protein parts of the molecules. In particular, the oxidation of spectrin and hemoglobin takes place [11, 13]. As a result, protein aggregation can occur, which also could locally change the membrane properties. It is the chain of the processes mentioned which could lead to the formation and development of local type A and B topological defects.

Spectrin oxidation could result in the disruption of the spectrin threads. The transformation of spectrin tetramers into dimmers leads to the expression of part of the membrane outside and, then, to the separation of vesicles from the cell. This is vesiculation [26, 27]. Type B defects could be the beginning of vesiculation: "vesiculation outside."

At the same time, the separation of tetramers and local impairments in the bond between spectrin and the bilayer could be the reason for a local dip of the lipid bilayer inside the cell. Thus, on the membrane surface, regions located below the membrane surface form. It is these regions that are type A defects of the membrane. These effects were observed in the study under exposure to ferriheme and furosemide [18, 19]. However, the parameters of the topological defects under the effect of the UV radiation were specific and differed from the characteristic defects of each of the exposures mentioned. We interpret this process of a

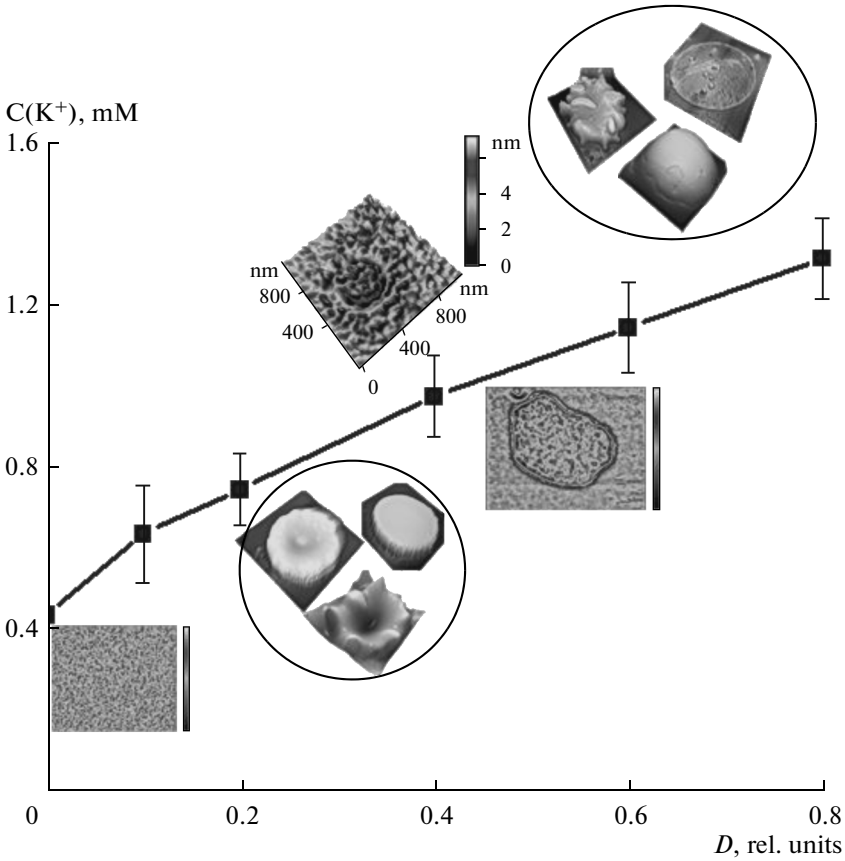

Fig. 6. Dependence of the concentration of extracellular potassium on the dose of UV radiation. AFM images of fragments of membrane nanostructure corresponding to the doses are shown.

local dip of the membrane inside the cell as "vesiculation inside" [19].

A change in the nanostructure of the erythrocyte membranes and their morphology leads to impaired rheological properties of blood and triggers an immune response.

CONCLUSIONS

In this study the images of the local defects in the nanostructure of the erythrocyte membranes, which were induced by the effect of the UV radiation on blood, were shown using AFM.

The cell membrane together with DNA is a critical target of ionizing radiation. The damage of biological membranes could change the functional state of the cell and be a triggering mechanism for the development of pathophysiological processes in the organism as a whole. An investigation of changes in the nanosurface of the erythrocyte membranes together with hematological and biochemical indices of blood is of importance for developing an optimal method of radiation therapy and sterilization of foodstuff and donor blood upon prolonged storage. This research is of scientific interest for developing scientific approaches and the implementation of methods of eliminating consequences of the ionizing radiation of blood and organism as a whole.

REFERENCES

1. H. Turker, "Potential effects of ultraviolet-C radiation on the mole rats (Spalaxleucodon), hematological values," Am. J. Mol. Biol. **2**, 235–240 (2013).
2. D. K. Myers and R. W. Bide, "Biochemical effects of X-irradiation on erythrocytes," Radiat. Res. **27**, 250–263 (1966).
3. R. Matthew and L. Drake, "Approaches for determining the effects of UV radiation on microorganisms in ballast water," Manage. Biol. Invasion **4**, 87–99 (2013).
4. J. B. Castelino, P. V. Holland, O. P. Jacobs, M. Lapidot, and M. Markovic, "Effects of ionizing radiation on blood and blood components: a survey," IAEA-TEC-DOC-934 (Vienna, 1997).
5. A. P. Kozlov, E. A. Krasavin, A. V. Boreiko, A. P. Chernyaev, P. Yu. Alekseeva, and U. A. Bliznyuk, "Investigation of erythrocyte membrane damage under the action of γ-radiation in a wide dose range using electroporation," Phys. Part. Nucl. Lett. **5**, 127 (2008).
6. A. P. Kozlov, E. A. Krasavin, A. V. Boreiko, A. P. Chernyaev, E. K. Kozlova, and A. M. Chernysh, "Investigation of erythrocyte membrane damage dur-

ing irradiation by accelerated boron ion beam," Med. Fiz., No. 1, 69–72 (2007).

7. U. A. Bliznyuk, E. K. Kozlova, L. I. Deev, A. G. Platonov, A. P. Chernyaev, A. M. Chernysh, P. Yu. Alekseeva, and A. P. Kozlov, "Investigation of depth distribution of radiation effect by accelerated electron beam passing in erythrocyte suspension using the electroporation method," Med. Fiz., No. 2, 67–70 (2007).
8. E. K. Manders and C. D. Manders, "Sterilization, stabilization and preservation of functional biologics," Patent Application Publ., US 2004/0126880 A1.
9. *Human Physiology*, Ed. by R. F. Schmidt and G. Thews (Springer, Berlin, Heidelberg, New York, 1983; Mir, Moscow, 2005), pp. 423–426.
10. Yu. B. Kudryashov and B. S. Berenfel'd, *Principles of Radiation Biophysics* (Mosk. Gos. Univ., Moscow, 1982) [in Russian].
11. E. K. Kozlova, A. M. Chernysh, A. P. Chernyaev, A. V. Bushueva, O. E. Gudkova, V. A. Sergunova, A. P. Kozlov, and Yu. S. Zhdankina, "Oxidation processes under the action of ultraviolet radiation on red blood cells," Med. Fiz., No. 2, 63–70 (2014).
12. H. L. Reddy, S. K. Doane, S. D. Keil, S. Marschner, and R. P. Goodrich, "Development of a riboflavin and ultraviolet light-based device to treat whole blood," Transfusion **53** (Suppl. 1), 131–136 (2013).
13. R. B. Misra, R. S. Ray, and R. K. Hans, "Effect of UVB radiation on human erythrocytes *in vitro*," Toxicol. *In vitro* **19**, 433–438 (2005).
14. E. Kozlova, A. Chernysh, V. Moroz, O. Gudkova, V. Sergunova, and A. Kuzovlev, "Atomic force microscope images of the nanostructure of red blood cells membrane under the action of ionizing radiation and other physicochemical influence," in *Proceedings of the Workshop on Physics Health in Europe* (CERN, 2010), p. 46.
15. V. V. Moroz, A. M. Chernysh, E. K. Kozlova, P. Y. Borshegovskaya, U. A. Bliznjuk, R. M. Rysaeva, and O. Y. Gudkova, "Comparison of red blood cell membrane microstructure after different physicochemical influences: atomic force microscope research," J. Crit. Care **25**, 539.e1–539.e12 (2010).
16. V. V. Moroz, A. M. Chernysh, E. K. Kozlova, V. A. Sergunova, O. E. Gudkova, M. S. Fedorova, A. K. Kirsanova, and I. S. Novoderzhkina, "Violations of erythrocyte membrane nanostructure during acute blood loss and their correction by perfluorocarbon emulsions," Obshch. Reanimatol. **7** (2), 5–9 (2011).
17. V. V. Moroz, A. K. Kirsanova, I. S. Novoderzhkina, E. K. Kozlova, P. Yu. Borshchegovskaya, U. A. Bliznyuk, V. V. Aleksandrin, and A. M. Chernysh, "Changes in erythrocyte membrane surface ultrastructure after blood loss and its correction by laser irradiation," Obshch. Reanimatol. **6** (2), 5–9 (2010).
18. E. K. Kozlova, A. M. Chernysh, V. V. Moroz, and A. N. Kuzovlev, "Analysis of nanostructure of red blood cells membranes by space fourier transform of AFM images," Micron **44**, 218–227 (2013).
19. E. Kozlova, A. Chernysh, V. Moroz, O. Gudkova, V. Sergunova, and A. Kuzovlev, "Transformation of membrane nanosurface of red blood cells under hemin action," Sci. Rep., 11 (2014).
20. V. V. Moroz, E. K. Kozlova, A. M. Chernysh, O. E. Gudkova, and A. V. Bushueva, "Transformation of erythrocyte membrane structure under hemin action," Obshch. Reanimatol., No. 6, 5–10 (2012).
21. A. M. Chernysh, E. K. Kozlova, V. V. Moroz, V. A. Sergunova, O. Y. Gudkova, and M. S. Fedorova, "Reversible zinc-induced injuries to erythrocyte membrane nanostructure," Bull. Exp. Biol. Med. **154**, 84–88 (2012).
22. L. Wielopolski and B. Ciesielski, "Boron dose determination for BNCT using Fricke and EPR dosimetry," in *Cancer Neutron Capture Therapy,* Ed. by Y. Mishima (Springer, US, 1996), pp. 467–471.
23. G. Bosman, M. Stappersa, and V. Novotny, "Changes in band 3 structure as determinants of erythrocyte integrity during storage and survival after transfusion," Blood Transfus. **8** (Suppl. 3), s48–s52 (2010).
24. V. V. Moroz, A. M. Golubev, A. M. Chernysh, E. K. Kozlova, V. Yu. Vasil'ev, O. E. Gudkova, V. A. Sergunova, and M. S. Fedorova, "Transformation of erythrocyte membrane surface structure during prolonged storage of donated blood," Obshch. Reanimatol. **8** (1), 5 (2012).
25. R. E. Jhonson and T. I. Quickenden, "Photolysis and radiolysis of water ice on outer solar system bodies," J. Geophys. Res. **102** (E5), 10985 (1997).
26. J. Cluitmans, P. Sens, and G. J. C. J. M. Bosman, "Cytoskeletal control of red blood cell shape: theory and practice of vesicle formation," in *Advances in Planar Lipid Bilayers and Liposomes*, Ed. by A. Leitmannova Liu and A. Iglić (Academic, Burlington, 2009), Vol. 10, pp. 95–119.
27. G. M. Wagner, D. T. Chiu, J. H. Qju, R. H. Heath, and B. H. Lubin, "Spectrin oxidation correlates with membrane vesiculation in stored RBCs," Blood **69**, 1777–1781 (1987).

Translated by E. Berezhnaya